



Protracted study on a real physical phenomenon generated by media inhomogeneities

Hassan Almusawa^a, Khalid K. Ali^b, Abdul-Majid Wazwaz^c, M.S. Mehanna^d, D. Baleanu^{e,f,g,*}, M.S. Osman^{h,**}

^a Department of Mathematics, College of Sciences, Jazan University, Jazan 45142, Saudi Arabia

^b Mathematics Department, Faculty of Science, Al-Azhar University, Nasr-City, Cairo, Egypt

^c Department of Mathematics, Saint Xavier University, Chicago, IL 60655, USA

^d Faculty of Engineering, MTI University, Cairo, Egypt

^e Department of Mathematics, Faculty of Arts and Sciences, Çankaya University, Öğretmenler Cad. 1406530, Ankara, Turkey

^f Institute of Space Sciences, Magurele, Bucharest, Romania

^g Department of Medical Research, China Medical University Hospita, China Medical University, Taichung, Taiwan

^h Department of Mathematics, Faculty of Science, Cairo University, Giza 12613, Egypt

ARTICLE INFO

Keywords:

Different analytical approaches

Traveling wave solutions

Numerical technique

ABSTRACT

In this work, we study the dynamical behavior for a real physical application due to the inhomogeneities of media via analytical and numerical approaches. This phenomenon is described by the 3D Date–Jimbo–Kashiwara–Miwa (3D-DJKM) equation. For analytical techniques, three different methods are performed to get hyperbolic, trigonometric and rational functions solutions. After that, the obtained solutions are graphically depicted through 2D- and 3D-plots and numerically compared via the finite difference algorithm to check the precision of the proposed methods.

Introduction

It is known that the study of higher-dimensional nonlinear PDEs (HD-NLPDEs) has been linked to a slew of important issues in fields like physical science, ecology, and engineering technology [1–7]. The explicit analytic solutions of HD-NLPDEs must be obtained in order to rummage into the complex mechanism for these models [8–11]. Many studies shed light on the exact solutions of HD-NLPDEs in recent years, such as the 2D-DJKM equation [12–18]:

$$u_{xxxxxy} + 4u_{xxy}u_x + 2u_{xxx}u_y + 6u_{xy}u_{xx} - au_{yyy} - 2\beta u_{xxt} = 0, \quad (1)$$

which explains how nonlinear dispersive waves propagate in inhomogeneous media, $u = u(x, y, t)$ represents the maximum extension for the waves measured from the equilibrium position. The coefficients of the last two terms of (1) are free parameters.

Wazwaz had developed the 2D-DJKM equation by adding the term $(ku_x + ru_y + su_z)_{xx}$ to become 3D-DJKM equation [19]. The new 3D-DJKM equation takes the form:

$$u_{xxxxxy} + 4u_{xxy}u_x + 2u_{xxx}u_y + 6u_{xy}u_{xx} - au_{yyy} - 2\beta u_{xxt} + (ku_x + ru_y + su_z)_{xx} = 0.$$

(2)

Wazwaz showed that (2) is integrable in the Painlevé sense and he gave the solution using Hirota's method [19].

In this work, three methods will be used to get abundant solutions to the 3D-DJKM equation, the first one is the $\exp(-\phi(\xi))$ expansion method [20–22], the second is the $(\frac{G'}{G})$ -expansion method [23–25] and the third one is the sine–Gordon expansion method [26–30]. Furthermore, we use a numerical technique, finite difference algorithm (FDA), to gain some numerical solutions [31,32]. The brief description of the article is provided as follows: We give the outlines for the three used techniques in Section “The methodologies”. We extend the implementations of the given methods to construct analytical solutions for the 3D-DJKM equation in Section “Applications”. The numerical solutions for that equation are introduced in Section “The finite difference algorithm (FDA)”. Some graphical illustrations are presented in Section “Graphical interpretations”. At the last, some closing results are stated in Section “Conclusion”.

* Corresponding author at: Department of Mathematics, Faculty of Arts and Sciences, Çankaya University, Öğretmenler Cad. 1406530, Ankara, Turkey.

** Corresponding author.

E-mail addresses: dumitru@cankaya.edu.tr (D. Baleanu), mofatzi@sci.cu.edu.eg, mofatzi@cu.edu.eg (M.S. Osman).

The methodologies

The exp(-φ(ξ)) expansion technique

Let us assume the following traveling wave equation in the form of PDE:

$$R(\Lambda, \Lambda_t, \Lambda_x, \Lambda_y, \Lambda_z, \Lambda_{xt}, \Lambda_{xx}, \Lambda_{yt}, \Lambda_{yy}, \Lambda_{xz}, \dots) = 0, \tag{3}$$

where $\Lambda = \Lambda(x, y, z, t)$.

- (i) Combining the free parameters x, y, z and t into one parameter ξ by using the following propagational wave transform:

$$\Lambda(x, y, z, t) = \Pi(\xi), \quad \xi = ax + by + dz - ct, \tag{4}$$

where a, b and d are constants and c is the speed of the wave. The transformation given by (4) changes (3) into an ordinary differential equation

$$\mathfrak{R}(\Pi, \Pi', \Pi'', \Pi''', \dots) = 0, \tag{5}$$

where \mathfrak{R} is a polynomial in Π and its derivatives.

- (ii) By applying the exp(-φ(ξ)) expansion technique, Eq. (5) has the following type of solutions:

$$\Pi(\xi) = \sum_{i=0}^N S_i (\exp(-\phi(\xi)))^i, \tag{6}$$

where $S_i (0 \leq i \leq N)$ are constants and

$$\phi'(\xi) = \exp(-\phi(\xi)) + \wp \exp(\phi(\xi)) + \vartheta. \tag{7}$$

Group 1: $\vartheta^2 - 4\wp > 0, \wp \neq 0,$

$$\phi(\xi) = \ln\left(\frac{-\sqrt{(\vartheta^2 - 4\wp)} \tanh\left(\frac{\sqrt{(\vartheta^2 - 4\wp)}}{2}(\xi + E)\right) - \vartheta}{2\wp}\right), \tag{8}$$

$$\phi(\xi) = \ln\left(\frac{-\sqrt{(\vartheta^2 - 4\wp)} \coth\left(\frac{\sqrt{(\vartheta^2 - 4\wp)}}{2}(\xi + E)\right) - \vartheta}{2\wp}\right), \tag{9}$$

where E is an integration constant.

Group 2: $\vartheta^2 - 4\wp < 0, \wp \neq 0,$

$$\phi(\xi) = \ln\left(\frac{\sqrt{(4\wp - \vartheta^2)} \tan\left(\frac{\sqrt{(4\wp - \vartheta^2)}}{2}(\xi + E)\right) - \vartheta}{2\wp}\right), \tag{10}$$

$$\phi(\xi) = \ln\left(\frac{\sqrt{(4\wp - \vartheta^2)} \cot\left(\frac{\sqrt{(4\wp - \vartheta^2)}}{2}(\xi + E)\right) - \vartheta}{2\wp}\right). \tag{11}$$

Group 3: $\vartheta^2 - 4\wp > 0, \wp = 0, \vartheta \neq 0,$

$$\phi(\xi) = -\ln\left(\frac{\vartheta}{\exp(\vartheta(\xi + E)) - 1}\right). \tag{12}$$

Group 4: $\vartheta^2 - 4\wp = 0, \wp \neq 0, \vartheta \neq 0,$

$$\phi(\xi) = \ln\left(-\frac{2(\vartheta(\xi + E) + 2)}{\vartheta^2(\xi + E)}\right). \tag{13}$$

Group 5: $\vartheta^2 - 4\wp = 0, \wp = 0, \vartheta = 0,$

$$\phi(\xi) = \ln(\xi + E). \tag{14}$$

- (iii) The value of $N > 0$ may be calculated through the balance technique of the highest derivative and the nonlinear term in Eq. (5). After that, we insert (6) into (5) and we equate all the coefficients of $(\exp(-\Phi(\xi)))^i, i = 0, 1, 2, \dots, N$ to zero to get an algebraic set of equations in terms of $S_0, \dots, S_N, \vartheta, \wp, a, b, c, d$ which can be directly solved. If we substitute the obtained values into Eq. (6), then we obtain the general form of solution for Eq. (3).

The (G'/G)-expansion technique

The $(\frac{G'}{G})$ -expansion approach can be used by applying the following techniques:

- (i) Assume that the general solution of Eq. (5) has the form:

$$\Pi(\xi) = \sum_{i=0}^N a_i \left(\frac{G'}{G}\right)^i, \tag{15}$$

where $G = G(\xi)$ is given by:

$$G''(\xi) + \vartheta G'(\xi) + \wp G(\xi) = 0, \tag{16}$$

where $a_i (i = 0, 1, 2, \dots, N), a_N \neq 0, \vartheta$ and \wp are constants.

- (ii) In (5), $N > 0$ can be calculated by using the balancing condition on Eq. (4).

- (iii) Eq. (16) has three different categories of solutions:

Group 1: Hyperbolic solution type, when $\vartheta^2 - 4\wp > 0,$

$$\frac{G'}{G} = \frac{-\vartheta}{2} + \frac{1}{2} \sqrt{\vartheta^2 - 4\wp} \frac{h_1 \sinh \frac{1}{2} \sqrt{\vartheta^2 - 4\wp} \xi + h_2 \cosh \frac{1}{2} \sqrt{\vartheta^2 - 4\wp} \xi}{h_1 \cosh \frac{1}{2} \sqrt{\vartheta^2 - 4\wp} \xi + h_2 \sinh \frac{1}{2} \sqrt{\vartheta^2 - 4\wp} \xi}, \tag{17}$$

Group 2: Trigonometric solution type, when $\vartheta^2 - 4\wp < 0,$

$$\frac{G'}{G} = \frac{-\vartheta}{2} + \frac{1}{2} \sqrt{4\wp - \vartheta^2} \frac{-h_1 \sin \frac{1}{2} \sqrt{4\wp - \vartheta^2} \xi + h_2 \cos \frac{1}{2} \sqrt{4\wp - \vartheta^2} \xi}{h_1 \cos \frac{1}{2} \sqrt{4\wp - \vartheta^2} \xi + h_2 \sin \frac{1}{2} \sqrt{4\wp - \vartheta^2} \xi}, \tag{18}$$

Group 3: Rational solution type, when $\vartheta^2 - 4\wp = 0,$

$$\frac{G'}{G} = \frac{-\vartheta}{2} + \frac{h_2}{h_1 + h_2 \xi}, \tag{19}$$

where h_1 and h_2 are the integration constants.

- (iv) Substituting (15) into (5), in the presence of (16), and equating all terms of $(\frac{G'}{G})^i, i = 0, 1, 2, \dots, N$ to zero, we reached to a system of equations in $a_i, \vartheta, \wp, a, b, c, d,$ that can be directly solved.

Sine-Gordon expansion Technique (SGET)

The well-known sine-Gordon equation is given by

$$\Lambda_{xx} - \Lambda_{tt} = m^2 \sin(\Lambda), \tag{20}$$

where $\Lambda = \Lambda(x, t)$ and m is a constant. By using the wave transformation $\Lambda(x, t) = \Pi(\xi), \xi = x - ct$ into (20), we get:

$$\Pi'' = \frac{m^2}{(1 - c^2)} \sin(\Pi). \tag{21}$$

By integrating (21) with respect to $\xi,$ we get:

$$\left[\left(\frac{\Pi}{2}\right)'\right]^2 = \frac{m^2}{(1 - c^2)} \sin^2\left(\frac{\Lambda}{2}\right), \tag{22}$$

where the integration constant is neglected. Let $\varpi(\xi) = \frac{\Lambda}{2}$ and $\kappa^2 = \frac{m^2}{(1 - c^2)},$ so (22) becomes:

$$\varpi' = \kappa \sin(\varpi). \tag{23}$$

Set $\kappa = 1$ in (23), we get:

$$\varpi' = \sin(\varpi). \tag{24}$$

Solving (24), we obtain two different relations as:

$$\sin(\varpi) = \sin(\varpi(\xi)) = \frac{2pe^\xi}{p^2 e^{2\xi} + 1} \Bigg|_{p=1} = \operatorname{sech}(\xi), \tag{25}$$

$$\cos(\varpi) = \cos(\varpi(\xi)) = \frac{p^2 e^{2\xi} - 1}{p^2 e^{2\xi} + 1} \Bigg|_{p=1} = -\tanh(\xi), \tag{26}$$

where $p \neq 0$ is an integral constant.

We assume the general solution of (5) has the form:

$$\Pi(\xi) = A_0 + \sum_{i=1}^N ((-\tanh(\xi))^{i-1} (B_i \operatorname{sech}(\xi) - A_i \tanh(\xi))). \tag{27}$$

Use (25) and (26), we get:

$$\Pi(w) = A_0 + \sum_{i=1}^N (\cos^{i-1}(\varpi))(B_i \sin(\varpi) + A_i \cos(\varpi)). \tag{28}$$

The positive integer N and the coefficients of $\sin^i(\varpi) \cos^i(\varpi)$ can be calculated by the same steps given the previous two methods.

Applications

Applying the transformation (4) into (2), we get:

$$6a^3 bu''(\xi)^2 + (a^3 k - b^3 \alpha + a^2(br + ds + 2c\beta))u'(\xi) + a^4 bu^{(3)}(\xi) = 0. \tag{29}$$

Integrating it twice, neglecting the new constants, we get:

$$3a^3 bu'(\xi)^2 + (a^3 k - b^3 \alpha + a^2(br + ds + 2c\beta))u(\xi) + a^4 bu^{(3)}(\xi) = 0. \tag{30}$$

Balancing $u^{(3)}(\xi)$ with $(u'(\xi)^2)$ gives $N = 1$.

Solutions using the $\exp(-\phi(\xi))$ expansion technique

From (6), we have:

$$u(\xi) = A_0 + A_1 \exp(-\phi(\xi)). \tag{31}$$

Substituting (31) into (30) with (7) and using the last item in our algorithm, we create the following system:

$$\begin{aligned} -a^3 k \theta A_1 - a^2 br \theta A_1 - a^2 ds \theta A_1 + b^3 \alpha \theta A_1 - 2a^2 c \beta \theta A_1 - a^4 b \theta^3 A_1 - 8a^4 b \theta \varphi A_1 \\ + 6a^3 b \theta \varphi A_1^2 = 0, \\ -a^3 k A_1 - a^2 br A_1 - a^2 ds A_1 + b^3 \alpha A_1 - 2a^2 c \beta A_1 - 7a^4 b \theta^2 A_1 - 8a^4 b \theta \varphi A_1 \\ + 3a^3 b \theta^2 A_1^2 + 6a^3 b \theta \varphi A_1^2 = 0, \\ -12a^4 b \theta A_1 + 6a^3 b \theta A_1^2 = 0, \\ -6a^4 b A_1 + 3a^3 b A_1^2 = 0, \\ -a^3 k \varphi A_1 - a^2 br \varphi A_1 - a^2 ds \varphi A_1 + b^3 \alpha \varphi A_1 - 2a^2 c \beta \varphi A_1 - a^4 b \theta^2 \varphi A_1 \\ - 2a^4 b \theta^2 \varphi A_1 + 3a^3 b \theta^2 \varphi A_1^2 = 0. \end{aligned}$$

The solution of the previous system is given by:

$$A_1 = 2a, d = \frac{-a^3 k - a^2 br + b^3 \alpha - 2a^2 c \beta - a^4 b \theta^2 + 4a^4 b \theta \varphi}{a^2 s}, \quad a, s \neq 0. \tag{32}$$

By substituting from (8) to (14) through (32) in (31) respectively, we get different solutions for (2) in the following shapes:

Group 1: $\vartheta^2 - 4\varphi > 0, \varphi \neq 0,$

$$u(x, y, z, t) = A_0 + \frac{4a\varphi}{-\vartheta - \sqrt{(\vartheta^2 - 4\varphi)} \tanh\left(\frac{\sqrt{(\vartheta^2 - 4\varphi)}}{2}(ax + by + dz - ct + E)\right)} \tag{33}$$

$$u(x, y, z, t) = A_0 + \frac{4a\varphi}{-\vartheta - \sqrt{(\vartheta^2 - 4\varphi)} \coth\left(\frac{\sqrt{(\vartheta^2 - 4\varphi)}}{2}(ax + by + dz - ct + E)\right)} \tag{34}$$

Group 2: $\vartheta^2 - 4\varphi < 0, \varphi \neq 0,$

$$u(x, y, z, t) = A_0 + \frac{4a\varphi}{-\vartheta + \sqrt{4\varphi - \vartheta^2} \tan\left(\frac{\sqrt{4\varphi - \vartheta^2}}{2}(ax + by + dz - ct + E)\right)} \tag{35}$$

$$u(x, y, z, t) = A_0 + \frac{4a\varphi}{-\vartheta + \sqrt{4\varphi - \vartheta^2} \cot\left(\frac{\sqrt{4\varphi - \vartheta^2}}{2}(ax + by + dz - ct + E)\right)} \tag{36}$$

Group 3: $\vartheta^2 - 4\varphi > 0, \varphi = 0, \vartheta \neq 0,$

$$u(x, y, z, t) = A_0 + \frac{2a\vartheta}{-1 + e^{\vartheta(ax+by+dz - a^3 k - a^2 br + b^3 \alpha - 2a^2 c \beta - a^4 b \theta^2 + 4a^4 b \theta \varphi) - ct + E}} \tag{37}$$

Group 4: $\vartheta^2 - 4\varphi = 0, \varphi \neq 0, \vartheta \neq 0,$

$$u(x, y, z, t) = A_0 - \frac{a\vartheta^2(ax + by + dz - ct + E)}{2 + \vartheta(ax + by + dz - ct + E)} \tag{38}$$

Group 5: $\vartheta^2 - 4\varphi = 0, \varphi = 0, \vartheta = 0,$

$$u(x, y, z, t) = A_0 + \frac{2a}{(ax + by + dz - a^3 k - a^2 br + b^3 \alpha - 2a^2 c \beta - a^4 b \theta^2 + 4a^4 b \theta \varphi) - ct + E} \tag{39}$$

Solutions using the $(\frac{G'}{G})$ -expansion method

According to (15), we have the solution form of (30) as:

$$u(\xi) = a_0 + a_1 \frac{G'}{G}, \tag{40}$$

substituting (40) into (30) and equating all terms with the same power of $\frac{G'}{G}$ to zero, we get:

$$\begin{aligned} -a^3 k \varphi a_1 - a^2 br \varphi a_1 - a^2 ds \varphi a_1 + b^3 \alpha \varphi a_1 - 2a^2 c \beta \varphi a_1 - a^4 b \theta^2 \varphi a_1 - 2a^4 b \theta^2 a_1 \\ + 3a^3 b \theta^2 a_1^2 = 0, \\ -a^3 k \theta a_1 - a^2 br \theta a_1 - a^2 ds \theta a_1 + b^3 \alpha \theta a_1 - 2a^2 c \beta \theta a_1 - a^4 b \theta^3 a_1 - 8a^4 b \theta \varphi a_1 \\ + 6a^3 b \theta \varphi a_1^2 = 0, \\ -12a^4 b \theta a_1 + 6a^3 b \theta a_1^2 = 0, \\ -6a^4 b a_1 + 3a^3 b a_1^2 = 0, \\ -a^3 k a_1 - a^2 br a_1 - a^2 ds a_1 + b^3 \alpha a_1 - 2a^2 c \beta a_1 - 7a^4 b \theta^2 a_1 - 8a^4 b \theta \varphi a_1 \\ + 3a^3 b \theta^2 a_1^2 + 6a^3 b \theta \varphi a_1^2 = 0. \end{aligned}$$

The algebraic solution of the previous system is given by:

$$a_1 = 2a, \quad d = \frac{-a^3 k - a^2 br + b^3 \alpha - 2a^2 c \beta - a^4 b \theta^2 + 4a^4 b \theta \varphi}{a^2 s}, \quad a, s \neq 0. \tag{41}$$

By substituting from (17) to (19) with (41) into (40) respectively, we get different types of solutions for (2) as:

Group 1: Hyperbolic solution type, when $\vartheta^2 - 4\varphi > 0,$

$$u(x, y, z, t) = a_0 + \left(-a\vartheta + a\sqrt{\vartheta^2 - 4\varphi} \frac{h_1 \sinh \frac{1}{2} \sqrt{\vartheta^2 - 4\varphi}(ax + by + dz - ct) + h_2 \cosh \frac{1}{2} \sqrt{\vartheta^2 - 4\varphi}(ax + by + dz - ct)}{h_1 \cosh \frac{1}{2} \sqrt{\vartheta^2 - 4\varphi}(ax + by + dz - ct) + h_2 \sinh \frac{1}{2} \sqrt{\vartheta^2 - 4\varphi}(ax + by + dz - ct)} \right), \tag{42}$$

Group 2: Trigonometric solution type, when $\vartheta^2 - 4\varphi < 0,$

$$u(x, y, z, t) = a_0 + \left(-a\vartheta + a\sqrt{4\varphi - \vartheta^2} \frac{-h_1 \sin \frac{1}{2} \sqrt{4\varphi - \vartheta^2}(ax + by + dz - ct) + h_2 \cos \frac{1}{2} \sqrt{4\varphi - \vartheta^2}(ax + by + dz - ct)}{h_1 \cos \frac{1}{2} \sqrt{4\varphi - \vartheta^2}(ax + by + dz - ct) + h_2 \sin \frac{1}{2} \sqrt{4\varphi - \vartheta^2}(ax + by + dz - ct)} \right), \tag{43}$$

Group 3: Rational solution type, when $\vartheta^2 - 4\varphi = 0,$

$$u(x, y, z, t) = a_0 + 2a \left(\frac{-\vartheta}{2} + \frac{h_2}{h_1 + h_2(ax + by + dz - ct)} \right), \tag{44}$$

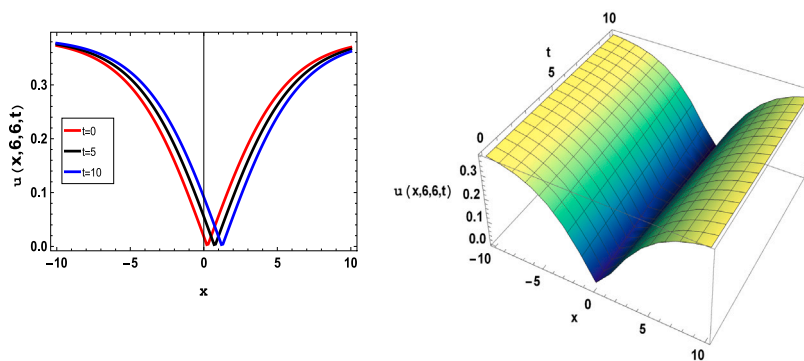


Fig. 1. Sketch of (33) in 2D and 3D charts.

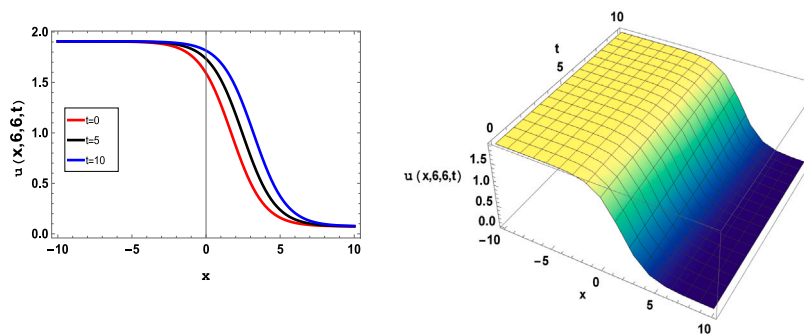


Fig. 2. Sketch of (42) in 2D and 3D charts.

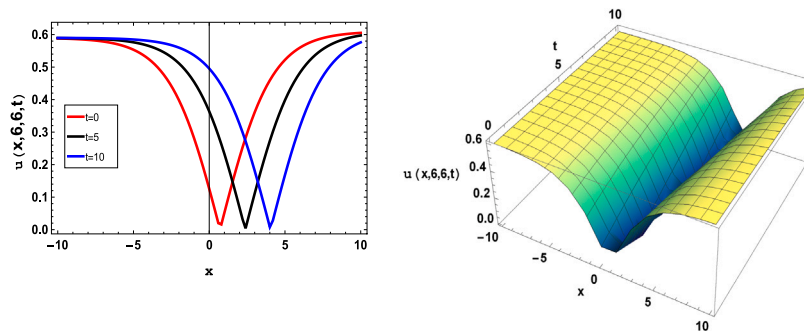


Fig. 3. Sketch of (47) in 2D and 3D charts.

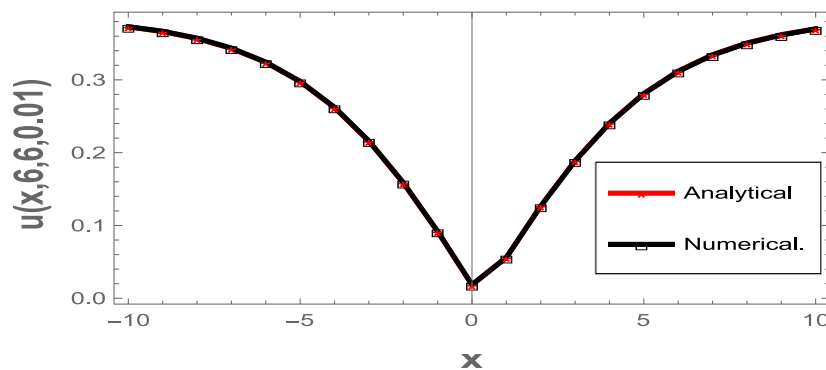


Fig. 4. Sketch of a comparison study for (33) when $\Delta t = 0.001, q = h = g = 1$.

Table 1
The numerical solutions for Eq. (33).

| x | Approx. Sol. | Anal. Sol. | Abs. error |
|-------|--------------|------------|----------------------------|
| -10.0 | 0.372921 | 0.372921 | 0.00000 |
| -8.0 | 0.357225 | 0.356767 | 4.58382 × 10 ⁻⁴ |
| -6.0 | 0.324404 | 0.323973 | 4.31517 × 10 ⁻⁴ |
| -4.0 | 0.262296 | 0.261892 | 4.03745 × 10 ⁻⁴ |
| -2.0 | 0.158887 | 0.158527 | 3.60051 × 10 ⁻⁴ |
| 0.0 | 0.018703 | 0.018378 | 3.25215 × 10 ⁻⁴ |
| 2.0 | 0.126411 | 0.126766 | 3.54310 × 10 ⁻⁴ |
| 4.0 | 0.240218 | 0.240626 | 4.07543 × 10 ⁻⁴ |
| 6.0 | 0.311571 | 0.312013 | 4.42584 × 10 ⁻⁴ |
| 8.0 | 0.350211 | 0.350682 | 4.70786 × 10 ⁻⁴ |
| 10.0 | 0.369981 | 0.369981 | 0.00000 |

Solution using Sine–Gordon expansion technique (SGET)

From (28), we have:

$$U(\varpi) = A_0 + B_1 \sin \varpi + A_1 \cos \varpi, \tag{45}$$

By substituting from (45) and (24) into (30) and repeating the steps above gives:

$$-a^3 k A_1 - a^2 b r A_1 - a^2 d s A_1 + b^3 \alpha A_1 - 2a^2 c \beta A_1 - 4a^4 b A_1 + 3a^3 b B_1^2 = 0,$$

$$a^3 k B_1 + a^2 b r B_1 + a^2 d s B_1 - b^3 \alpha B_1 + 2a^2 c \beta B_1 + a^4 b B_1 = 0,$$

$$6a^4 b A_1 + 3a^3 b A_1^2 - 3a^3 b B_1^2 = 0,$$

$$-4a^4 b B_1 - 6a^3 b A_1 B_1 = 0.$$

This system has the following solutions

$$A_1 = -2a, B_1 = 0, d = \frac{-4a^4 b - a^3 k - a^2 b r + b^3 \alpha - 2a^2 c \beta}{a^2 s}, \quad a, s \neq 0. \tag{46}$$

Hence, we achieve the required solution:

$$u(x, y, z, t) = A_0 - 2a \tanh(ct - ax - by) - \frac{z(-4a^4 b - a^3 k - a^2 b r + b^3 \alpha - 2a^2 c \beta)}{a^2 s}. \tag{47}$$

The finite difference algorithm (FDA)

Here, we introduce the following approximations [31,32]:

$$\begin{aligned} u_t &\simeq \frac{\varrho_{\bar{r},\bar{s},l,m+1} - \varrho_{\bar{r},\bar{s},l,m}}{\Delta t} \\ u_x &\simeq \frac{\varrho_{\bar{r}+1,\bar{s},l,m} - \varrho_{\bar{r}-1,\bar{s},l,m}}{2h}, \\ u_{xx} &\simeq \frac{\varrho_{\bar{r}-1,\bar{s},l,m} + \varrho_{\bar{r}+1,\bar{s},l,m} - 2\varrho_{\bar{r},\bar{s},l,m}}{h^2}, \\ u_y &\simeq \frac{\varrho_{\bar{r},\bar{s}+1,l,m} - \varrho_{\bar{r},\bar{s}-1,l,m}}{2q}, \\ u_{yy} &\simeq \frac{\varrho_{\bar{r},\bar{s}-1,l,m} + \varrho_{\bar{r},\bar{s}+1,l,m} - 2\varrho_{\bar{r},\bar{s},l,m}}{q^2}, \\ u_{xxt} &\simeq \frac{1}{h^2 \Delta t} (\varrho_{\bar{r}-1,\bar{s},l,m+1} - 2\varrho_{\bar{r},\bar{s},l,m+1} + \varrho_{\bar{r}+1,\bar{s},l,m+1} \\ &\quad - (\varrho_{\bar{r}-1,\bar{s},l,m} - 2\varrho_{\bar{r},\bar{s},l,m} + \varrho_{\bar{r}+1,\bar{s},l,m})), \\ u_z &\simeq \frac{\varrho_{\bar{r},\bar{s},l+1,m} - \varrho_{\bar{r},\bar{s},l-1,m}}{2g}, \\ u_{xz} &\simeq \frac{\varrho_{\bar{r}-1,\bar{s},l,m} + \varrho_{\bar{r}+1,\bar{s},l,m} - 2\varrho_{\bar{r},\bar{s},l,m}}{h^2}, \\ &\vdots \end{aligned} \tag{48}$$

We mention that u and $\varrho_{\bar{r},\bar{s},l,m}$ are the exact and numerical solutions at $(x_{\bar{r}}, y_{\bar{s}}, z_l, t_m)$, respectively. Plugging (48) into (1), we get a difference equations system which is used to get the numerical values of $\varrho_{\bar{r},\bar{s},l,m}$.

Table 2
The numerical solutions for Eq. (42).

| x | Approx. Sol. | Anal. Sol. | Abs. error |
|-------|--------------|------------|----------------------------|
| -10.0 | 1.90648 | 1.90648 | 0.00000 |
| -8.0 | 1.90686 | 1.90627 | 5.96850 × 10 ⁻⁴ |
| -4.0 | 1.90270 | 1.89687 | 5.83141 × 10 ⁻³ |
| 0.0 | 1.60044 | 1.59230 | 8.13237 × 10 ⁻³ |
| 2.0 | 0.86436 | 0.87268 | 8.31876 × 10 ⁻³ |
| 6.0 | 0.09554 | 0.08786 | 7.68164 × 10 ⁻³ |
| 8.0 | 0.08373 | 0.07926 | 4.47177 × 10 ⁻³ |
| 10.0 | 0.07441 | 0.07441 | 0.00000 |

Table 3
The numerical solutions for Eq. (47).

| x | Approx. sol. | Anal. Sol. | Abs. error |
|-------|--------------|------------|----------------------------|
| -10.0 | 0.58812 | 0.58812 | 0.00000 |
| -8.0 | 0.58379 | 0.58381 | 2.00080 × 10 ⁻⁵ |
| -6.0 | 0.56964 | 0.56969 | 5.07396 × 10 ⁻⁵ |
| -4.0 | 0.52505 | 0.52512 | 6.34303 × 10 ⁻⁵ |
| -2.0 | 0.39855 | 0.39860 | 5.18311 × 10 ⁻⁵ |
| 0.0 | 0.12607 | 0.12618 | 1.14084 × 10 ⁻⁴ |
| 2.0 | 0.22195 | 0.22187 | 8.32552 × 10 ⁻⁵ |
| 4.0 | 0.45898 | 0.45895 | 2.81465 × 10 ⁻⁵ |
| 6.0 | 0.56014 | 0.56012 | 2.51879 × 10 ⁻⁵ |
| 8.0 | 0.59452 | 0.59452 | 3.07044 × 10 ⁻⁵ |
| 10.0 | 0.60529 | 0.60529 | 0.00000 |

The numerical outcomes

Here, the numerical solutions for Eq. (2) are introduced. Table 1 shows the numerical and analytical solutions for (33) at $\alpha = 0.2, \beta = 0.1, a = 5, b = 4, c = 0.5, a_0 = 0.5, r = 0.1, k = 0.4, s = 0.3, E = 0.001, \vartheta = 0.1, \wp = 0.001, \theta = -0.1$. While Fig. 4 contains the same analysis for (33) when $\Delta t = 0.001, q = h = g = 1$.

The same comparison in Table 1 is investigated in Table 2 for the solution (42) at $\alpha = 0.1, \beta = 0.1, a = 2, b = 7, c = 0.3, a_0 = 0.01, r = 0.4, k = 0.7, s = 0.2, \vartheta = 0.5, \wp = 0.01, \theta = 0.4, h_1 = 0.4, h_2 = 0.1$. Fig. 5 shows the same analysis for (42) when $\Delta t = 0.001, q = h = g = 1$.

Similarly, Table 3 discusses the solution (47) at $\alpha = 0.5, \beta = 0.4, a = 0.3, b = 0.3, c = 0.1, a_0 = 0.01, r = 0.1, k = 0.01, s = 0.2, \theta = 0.1$. Furthermore, Fig. 6 gives the analytical and numerical solutions for (47) when $\Delta t = 0.001, q = h = g = 1$.

Graphical interpretations

In this part, some figures in 2D- and 3D-plots are presented to illustrate the behavior for some of the obtained solutions. Some of them are sketched in Figs. 1–3 and the effectiveness of the used approaches being compared to the solutions gained in [19]. In Fig. 1, the solution (33) is investigated at $\alpha = 0.2, \beta = 0.1, a = 5, b = 4, c = 0.5, a_0 = 0.5, r = 0.1, k = 0.4, s = 0.3, E = 0.001, \vartheta = 0.1, \wp = 0.001, \theta = -0.1$. Graph of (42) at $\alpha = 0.1, \beta = 0.1, a = 2, b = 7, c = 0.3, a_0 = 0.01, r = 0.4, k = 0.7, s = 0.2, \vartheta = 0.5, \wp = 0.01, \theta = 0.4, h_1 = 0.4, h_2 = 0.1$ is stated in Fig. 2. Finally, we presented the graph of (47) at $\alpha = 0.5, \beta = 0.4, a = 0.3, b = 0.3, c = 0.1, a_0 = 0.01, r = 0.1, k = 0.01, s = 0.2, \theta = 0.1$ in Fig. 3. Moreover, some plots for approximate solutions are introduced in Figs. 4–6.

Conclusion

We have obtained different types of solutions for the 3D-DJMKM equation. These solutions are derived by three different analytical approaches. Among the obtained solutions: the singular, periodic, hyperbolic, rational wave solutions and other different types. The FDA is used to deal with the equation numerically and the accuracy of

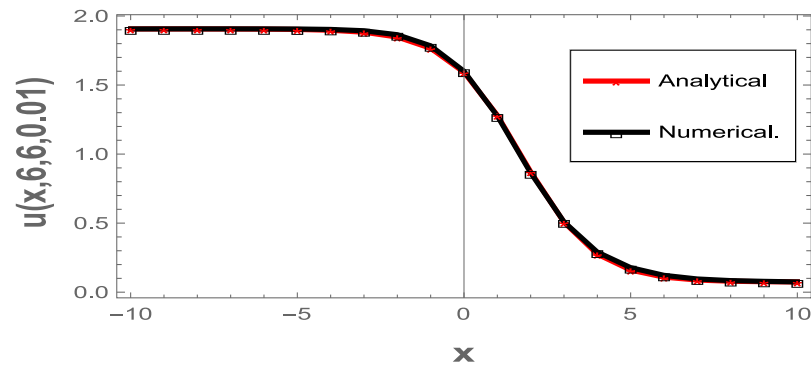


Fig. 5. Sketch of a comparison study for (42) when $\Delta t = 0.001, q = h = g = 1$.

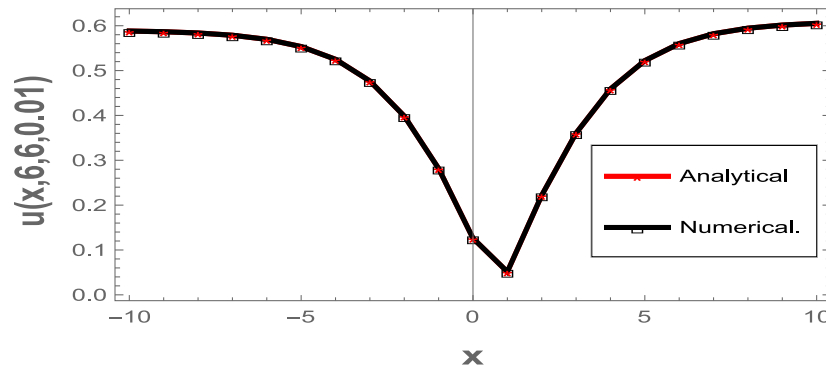


Fig. 6. Sketch of a comparison study for (47) when $\Delta t = 0.001, q = h = g = 1$.

our findings is demonstrated through the use of appropriate tables and figures that verified the effectiveness of the procedures employed. In addition to the other known results in the literature, the paper contributes new analytical and numerical results.

CRediT authorship contribution statement

Hassan Almusawa: Conceptualization, Formal analysis, Methodology, Software, Writing – review & editing. **Khalid K. Ali:** Data curation, Formal analysis, Methodology, Resources, Software, Writing – original draft. **Abdul-Majid Wazwaz:** Conceptualization, Investigation, Project administration, Supervision, Visualization, Writing – review & editing. **M.S. Mehanna:** Data curation, Investigation, Methodology, Resources, Validation, Writing – original draft. **D. Baleanu:** Conceptualization, Funding acquisition, Project administration, Resources, Supervision, Validation, Writing – review & editing. **M.S. Osman:** Conceptualization, Formal analysis, Funding acquisition, Methodology, Project administration, Software, Supervision, Writing – review & editing.

Declaration of competing interest

The authors declare that they have no known competing financial interests or personal relationships that could have appeared to influence the work reported in this paper.

References

- [1] Abdel-Gawad HI, Osman MS. On the variational approach for analyzing the stability of solutions of evolution equations. *Kyungpook Math J* 2013;53(4):661–80.
- [2] Kumar S, Almusawa H, Hamid I, Akbar MA, Abdou MA. Abundant analytical soliton solutions and evolutionary behaviors of various wave profiles to the chaffee-infante equation with gas diffusion in a homogeneous medium. *Results Phys* 2021;30:104866.
- [3] Osman MS, Machado JAT. New nonautonomous combined multi-wave solutions for $(2 + 1)$ -dimensional variable coefficients KdV equation. *Nonlinear Dynam* 2018;93(2):733–40.
- [4] Osman MS, Abdel-Gawad HI, El Mahdy MA. Two-layer-atmospheric blocking in a medium with high nonlinearity and lateral dispersion. *Results Phys* 2018;8:1054–60.
- [5] Osman MS. On multi-soliton solutions for the $(2 + 1)$ -dimensional breaking soliton equation with variable coefficients in a graded-index waveguide. *Comput Math Appl* 2018;75(1):1–6.
- [6] Osman MS, Almusawa H, Tariq KU, Anwar S, Kumar S, Younis M, Ma WX. On global behavior for complex soliton solutions of the perturbed nonlinear Schrödinger equation in nonlinear optical fibers. *J Ocean Eng Sci* 2021. <http://dx.doi.org/10.1016/j.joes.2021.09.018>.
- [7] Almusawa H, Nur Alam M, Fayz-Al-Asad M, Osman MS. New soliton configurations for two different models related to the nonlinear Schrödinger equation through a graded-index waveguide. *AIP Adv* 2021;11(6):065320.
- [8] Zhang L, Khalique CM. Traveling wave solutions and infinite-dimensional linear spaces of multiwave solutions to jimbo–miwa equation. *Abstr Appl Anal* 2014;2014:7. Article ID 963852.
- [9] Osman MS, Inc M, Liu JG, Hosseini K, Yusuf A. Different wave structures and stability analysis for the generalized $(2 + 1)$ -dimensional Camassa–Holm–Kadomtsev–Petviashvili equation. *Phys Scr* 2020;95(3):035229.
- [10] Alam MN, Osman MS. New structures for closed-form wave solutions for the dynamical equations model related to the ion sound and Langmuir waves. *Commun Theor Phys* 2021;73(3):035001.
- [11] Abdul Kayum M, Ara S, Osman MS, Akbar MA, Gepreel KA. Onset of the broad-ranging general stable soliton solutions of nonlinear equations in physics and gas dynamics. *Results Phys* 2021;20:103762.
- [12] Ismael HF, Bulut H, Park C, Osman MS. M-lump, N-soliton solutions, and the collision phenomena for the $(2 + 1)$ -dimensional Date–Jimbo–Kashiwara–Miwa equation. *Results Phys* 2020;19:103329.
- [13] Wazwaz AM. $(2 + 1)$ -dimensional time-dependent Date–Jimbo–Kashiwara–Miwa equation: Painlevé integrability and multiple soliton solutions. *Comput Math Appl* 2020;79(4):1145–9.
- [14] Karaagac B. Application of the improved $\tan(\phi(\xi)/2)$ -expansion method for solving date–Jimbo–Kashiwara–Miwa equation. *New Trends Math Sci* 2019;7(1):90–7.
- [15] Adem AR, Yildirim Y, Yaşar E. Complexiton solutions and soliton solutions: $(2 + 1)$ -dimensional Date–Jimbo–Kashiwara–Miwa equation. *Pramana J Phys* 2019;92:36.
- [16] Liu HZ. An equivalent form for the $\exp(-\phi(\xi))$ -expansion method. *Japan J Ind Appl Math* 2018;35(3):1153–61.
- [17] Adem AR, Yildirim Y, Yaşar E. Complexiton solutions and soliton solutions: $(2 + 1)$ -dimensional-date-jimbo-kashiwara-miwa equation. *Pramana J Phys* 2019;92:36.

- [18] Yuan YQ, Tian B, Sun WR, Chai J, Liu L. Wronskian and grammian solutions for a (2+1)-dimensional Date-Jimbo-Kashiwara-Miwa equation. *Comput Math Appl* Int J 2017;74(4):873–9.
- [19] Wazwaz AM. New (3+1)-dimensional date-jimbo-kashiwara-miwa equations with constant and time-dependent coefficients: Painlevé integrability. *Phys Lett A* 2020;384(32):126787.
- [20] Islam SMR. Applications of the $\exp(-\phi(\xi))$ -expansion method to find exact traveling wave solutions of the benney-luke equation in mathematical physics. *Amer J Appl Math* 2015;3(3):100–5.
- [21] Islam MR, Roshid HO. Application of $\exp(-\phi(\xi))$ expansion method for Tzitzeica type nonlinear evolution equations. *J Found Appl Phys* 2017;4(1):8–18.
- [22] Akbar MA, Ali NHM. Solitary wave solutions of the fourth order Boussinesq equation through the $\exp(-\phi(\xi))$ expansion method. *Springer Plus* 2014;3:344.
- [23] Taha WM, Noorani MSM. Explicit solutions for couple higher order nonlinear Schrödinger equation by $(\frac{G'}{G})$ -expansion method. *AIP Conf Proc* 2013;1571:980.
- [24] Naher H, Abdullah FA. The basic $(\frac{G'}{G})$ -expansion method for the fourth order Boussinesq equation. *Appl Math* 2012;3:1144–52.
- [25] Zayed EME, Al-Joudi S. The traveling wave solutions for nonlinear partial differential equations using the $(\frac{G'}{G})$ -expansion method. *Int J Nonlinear Sci* 2009;8(4):435–47.
- [26] Ali KK, Osman MS, Abdel-Aty M. New optical solitary wave solutions of Fokas-Lenells equation in optical fiber via Sine-Gordon expansion method. *Alexand Eng J* 2020;59:1191–6.
- [27] Ali KK, Wazwaz AM, Osman MS. Optical soliton solutions to the generalized nonautonomous nonlinear Schrödinger equations in optical fibers via the sine-Gordon expansion method. *Optik* 2020;208:164132.
- [28] Kumar D, Hosseini K, Samadani F. The sine-Gordon expansion method to look for the traveling wave solutions of the Tzitzeica type equations in nonlinear optics. *Optik* 2017;149:439–46.
- [29] Ismael HF, Bulut H, Baskonus HM. Optical soliton solutions to the Fokas-Lenells equation via sine-Gordon expansion method and $(m+(G'/G))$ -expansion method. *Pramana J Phys* 2020;94:35.
- [30] Kundu PR, Almusawa H, Fahim MRA, Islam ME, Akbar MA, Osman MS. Linear and nonlinear effects analysis on wave profiles in optics and quantum physics. *Results Phys* 2021;23:103995.
- [31] Raslan KR, Ali KK. Numerical study of MHD-duct flow using the two-dimensional finite difference method. *Appl Math Inf Sci* 2020;14:1–5.
- [32] EL-Danaf TS, Raslan KR, Ali KK. New numerical treatment for the generalized regularized long wave equation based on finite difference scheme. *Int J Soft Comput Eng* 2014;4:16–24.